Available online at www.sciencedirect.com
ScienceDirect
Medical Engineering & Physics 29 (2007) 1019–1029
Medical Engineering & Physics
www.elsevier.com/locate/medengphy

Technical note

Human voluntary activity integration in the control of a standing-up rehabilitation robot: A simulation study

Roman Kamnik*, Tadej Bajd

University of Ljubljana, Faculty of Electrical Engineering, Tržaška 25, 1001 Ljubljana, Slovenia

Received 7 October 2004; received in revised form 19 September 2006; accepted 24 September 2006

Abstract

The paper presents a novel control approach for the robot-assisted motion augmentation of disabled subjects during the standing-up manoeuvre. The main goal of the proposal is to integrate the voluntary activity of a person in the control scheme of the rehabilitation robot. The algorithm determines the supportive force to be tracked by a robot force controller. The basic idea behind the calculation of supportive force is to quantify the deficit in the dynamic equilibrium of the trunk. The proposed algorithm was implemented as a Kalman filter procedure and evaluated in a simulation environment. The simulation results proved the adequate and robust performance of "patient-driven" robot-assisted standing-up training. In addition, the possibility of varying the training conditions with different degrees of the subject's initiative is demonstrated.

Keywords: Rehabilitation robotics; Human–robotic interaction; Standing-up; Voluntary control

1. Introduction

Rising from a chair is a common, however demanding, activity of daily living. Disabled persons and the elderly often have difficulty when rising to a standing position. To compensate for the lack of lifting forces produced by muscles, a disabled person usually practices an adapted approach to the standing-up manoeuvre. Normally, the upper extremities take over the body weight lifting role. This requires a fit upper body. Additionally, in patients with lesions of the CNS, the standing-up exercise can be facilitated with the help of functional electrical stimulation (FES) evoking muscle contractions in the paralyzed extremities [1]. In clinical praxis, the knee extensors (quadriceps muscle groups) are stimulated to elicit moments in the knee joints [2].

When training a disabled subject to adapt to a new standing-up approach, the trainee needs to be, in numerous repetitions, restrained in a position trajectory and adequately supported to maintain postural stability. Furthermore, investigating new FES control approaches requires feedback to evaluate the effects of improvements. Training of standing-up is usually performed by the manual support of physiotherapists using also different mechanical aids. The back sled and seesaw construction are typical examples [3,4]. Mechanical aids are usually constructed as counterweight-based passive devices intended to aid the subject and assure his stability. None of the devices provides feedback information about the rising process or the capability of motion trajectory programming.

For these reasons, we have developed the standing-up robot-assistive device [5]. The device is designed as a three DOF mechanism driven by an electrohydraulic servosystem with a standard bike seat mounted at the end-effector. The disabled person is during robot-assisted standing-up supported under the buttocks, while the seat is moving in the subject's sagittal plane. The robot configuration allows the subject to actively participate in rising. In addition, the sensory system implemented in the robot device provides information about the standing-up parameters, making possible the assessment and evaluation of the human motion and therapeutic benefits of exercising.

* Corresponding author. Tel.: +386 1 4768 355; fax: +386 1 4768 239.
E-mail addresses: roman.kamnik@robo.fe.uni-lj.si (R. Kamnik), tadej.bajd@robo.fe.uni-lj.si (T. Bajd).

1350-4533/$ – see front matter © 2006 IPEM. Published by Elsevier Ltd. All rights reserved.
doi:10.1016/j.medengphy.2006.09.012

The robot controller allows different modes of operation. The robot device can operate either in a position control mode that provides tracking of the desired motion trajectory, in an impedance control mode that in addition to position tracking modulates the robot end-point dynamic behavior (stiffness, damping and inertia), or in a force control mode that assures application of the desired supportive force to the subject. In the position control mode, the robot can be considered as a pure position source with high impedance that imposes the motion of the subject's pelvis segment. Since no interaction control is involved in this regime, high man–machine interaction forces can occur. As an upgrade of position control, the impedance controller can provide smoother interaction since the robot while tracking the desired motion trajectory acts also as a predetermined dynamic system, for example, a mass-spring-damper system [6,7]. Because of this feature the impedance control is commonly utilized in rehabilitation robotics. Neither of the above approaches allow the rising subject in robot-assisted standing-up training to voluntarily control the standing-up maneuver. However, the incorporation of voluntary activity and control into motion augmentation training is crucial for progress of rehabilitation process. The force control approach enables an explicit control of the interaction force between the robot and the subject. Operation of the robot in this mode can provide the exact extent of support in each instant of rising. This approach has a potential for incorporation of the voluntary activity into the robot control, since the supportive force can be applied regarding the subject's action.

Two control approaches that account for voluntary activity in standing-up have been developed for controlling the FES systems utilized in persons with completely paralyzed lower extremities. Similar to robot-assisted standing-up, in FES-assisted standing-up of a paraplegic person, two systems are interacting: the upper body, whose motion is under voluntary control, and the lower body, whose motion is under the artificial control of FES. A "patient-driven motion reinforcement" (PDMR) algorithm [8] employs an inverse dynamic model of the human body to determine the joint torques in the lower extremities with the objective of preserving the motion initiated by the subject. An assessment of body motion kinematics is required in this approach. In [9] a "Control by Handle REactions of Leg Muscle Stimulation" (CHRELMS) algorithm was introduced by which the joint torques in the lower extremities were determined in accordance with arm reaction forces. In this approach, quasi-static conditions in standing-up were assumed and the upper trunk (also incorporating the head and arms) was considered as a free body. Joint torques in the lower extremities were determined with the goal of assuring the static equilibrium of the trunk. Implementation of the CHRELMS algorithm requires an assessment of body motion kinematics and handle reactions.

In this paper, the algorithm for the control of a standing-up rehabilitation robot is presented based on the idea of CHRELMS. The CHRELMS approach is, in our proposal, upgraded to be applicable for robot control that can account for fast dynamic motion and the voluntary contributions from the upper as well as lower extremities. The robot is supposed to operate in an explicit force control mode, while the desired human–robot interaction force is determined in a way that the dynamic equilibrium of the trunk segment is assured. We named the approach "patient-driven robot-assisted motion augmentation" (PDRAMA).

The paper is organized as follows. In Section 2, the mechanical design of the standing-up robot device and its control system are described. Section 3 presents the control approach proposed for patient-driven robot-supported standing-up training—PDRAMA. In Section 4, the algorithm is evaluated by means of simulations. The simulation results are compared with the results of the actual standing-up of a paraplegic subject facilitated by the robot device operating in position control mode. In Section 7, the advancements of the proposed technology are discussed.

2. Standing-up robot-assistive device

In the standing-up manoeuvre, the upper body can be considered as restricted to three degrees of freedom of motion. It moves vertically and horizontally in the sagittal plane, while changing its orientation in the antero-posterior direction. Thus, it can be reasonably assumed that the majority of subjects who are unable to stand-up (elderly, people with paraplegia or even some tetraplegic patients) will be able to control their upper body orientation by means of arm support. In this respect, an active mechanical system supporting the rising subject only under the buttocks, and in this way imposing the subject's pelvis trajectory and relieving the body weight, would be sufficient to transfer the human body from sitting to standing position. The novel robot device, developed according to the above criteria, is presented in Fig. 1.

The robot-assistive device is a three DOF mechanism which, in its way of supporting the subject, resembles half of a seesaw. The disabled subject sits on a standard bike seat mounted at the robot end-effector. Positioning of the end-effector is accomplished by positioning of two robot segments. The first segment is rotating around its axis on the robot base, while the second translational segment is moving longitudinally along the first segment. Both segments are driven by linear hydraulic actuators. At the robot end-effector, the orientational mechanism is mounted, assuring horizontal seat orientation in any robot position. Constant seat orientation is maintained by a passive hydraulic bilateral mechanism. The hydraulic bilateral system consists of two cylinders, master and slave, with the master piston coupled to the driving first robot segment. Under the seat mechanism, the six axis JR3 force/torque sensor (JR3 Inc., Woodland, USA) is mounted in order to assess the contact force between the robot end-point and the rising subject. In this manner, subject–machine interaction, and hence the robot assistance to the standing-up process, can be assessed and controlled on-line.

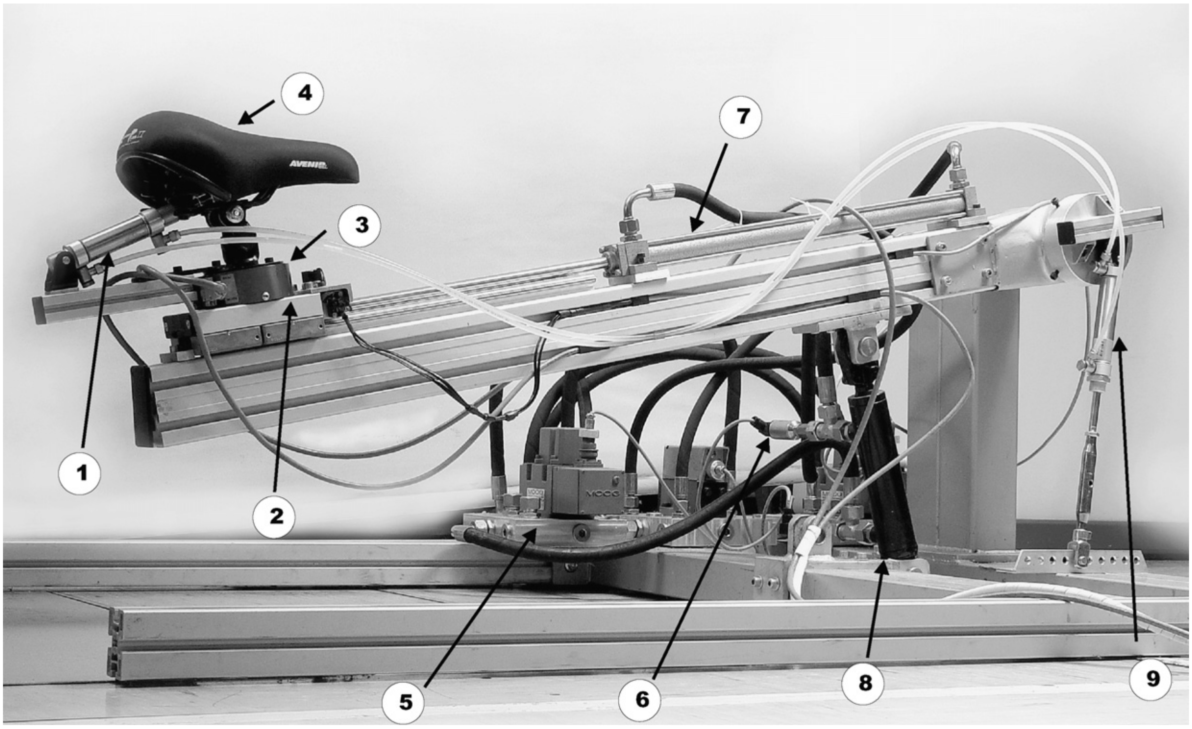

Fig. 1. Standing-up robot-assistive device: (1) seat orientation bilateral servo slave cylinder; (2) robot end-effector; (3) force sensor; (4) seat; (5) servo valves; (6) pressure sensors; (7) translational DOF hydraulic actuator; (8) rotational DOF hydraulic actuator; (9) seat orientation bilateral servo master cylinder.

The robot mechanism is driven by the electrohydraulic servosystem. The system is powered by a hydraulic pump providing a pressure of 50 bar and hydraulic current of 1 l/s. The pump performance allows a maximal speed of the robot end-effector up to 2 m/s. The current-driven Moog 062-234 servovalve (Moog Inc., New York, USA) is used to control the pressure difference applied to the linear hydraulic cylinder driving the translating link. Furthermore, two Moog D641-3 servovalves with incorporated electronics form a hydraulic arrangement, which drives the rotating link. This arrangement enables individual chamber pressure control in the hydraulic cylinder [10]. In this way, two operational modes are provided. In the position control mode, the system accomplishes the desired motion trajectory regardless of the interaction between the subject and the robot, while in the force control mode, explicit control of interaction force is possible.

The hydraulic servosystem is controlled by a computer system built on a 1 GHz PC Pentium III platform. On the platform, the RTLinux v. 3.1 real time operating system is running at a constant sampling rate of 2 kHz. Two PCI interface boards are used to interface with the external hardware.

3. Human voluntary activity integration in the control of a standing-up robot—PDRAMA approach

As an alternative to position or impedance control, we are proposing a control approach integrating human voluntary activity into the robot control scheme. The robot is supposed to operate in a force control mode, while the force reference is determined according to the rising subject's activity. In this way, the artificial robot controller is integrated into the control actions of the intact neuromuscular system of the subject. Hand and foot support forces are used to characterize the subject's volition and are thus used as feedback to the controller. The basic idea behind the calculation of the reference force is to quantify the deficit in the force and moment equilibrium of the trunk. Namely, if we simplify the situation and consider the subject's head, arms and trunk (HAT segment) as a rigid body, the balance equations for the forces and moments acting on this body segment can be defined. During motion, the HAT segment is supported by the lower and upper extremities in the hip and shoulder joints. The contributions of shoulder joint force $\vec{F}_{\text{sh}}$, shoulder joint moment $\vec{M}_{\text{sh}}$, hip joint force $\vec{F}_{\text{hip}}$, hip joint moment $\vec{M}_{\text{hip}}$ and the inertial contributions due to translational and angular accelerations are illustrated in Fig. 2. Assuming human body symmetry during rising, the HAT motion can be considered as planar, constrained to the subject's sagittal plane.

If the joint reactions and the HAT motion are known, the HAT balance can be determined and thus postural stability assured by applying additional external force to the HAT segment. Additional force $\vec{F}_{\text{robo}}$ is, in robot-assisted standing-up, contributed by the robot device supporting the HAT segment near the hip joints. Following the Newton–Euler approach to analyzing rigid body motion dynamics, the force and moment

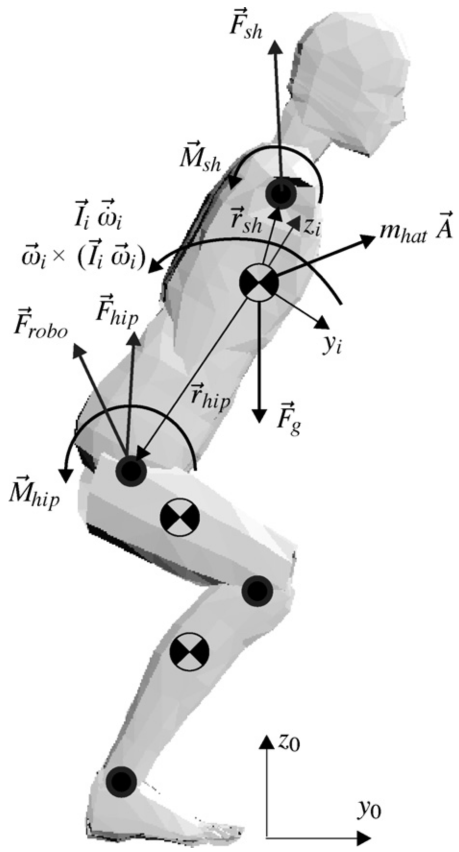

Fig. 2. Forces and moments in robot-assisted standing-up acting to the HAT segment.

balance equations for the HAT segment can be defined as

$$\vec{F}_{\rm hip} + \vec{F}_{\rm sh} + \vec{F}_{\rm g} + \vec{F}_{\rm robo} = m_{\rm hat}\vec{A} \tag{1}$$

$$\vec{M}_{\rm hip} + \vec{M}_{\rm sh} + \vec{F}_{\rm hip} \times \vec{r}_{\rm hip} + \vec{F}_{\rm sh} \times \vec{r}_{\rm sh} + \vec{F}_{\rm robo} \times \vec{r}_{\rm hip} = \frac{{\rm d}(\vec{I}_0\,\vec{\omega}_0)}{{\rm d}t} \tag{2}$$

In (1) and (2) the vectors $\vec{r}_{\rm hip}$ and $\vec{r}_{\rm sh}$ describe the position of the hip and shoulder joints with respect to the HAT center of mass. $\vec{F}_{\rm g}$ stands for gravitational force. The parameters $m_{\rm hat}$, $\vec{I}_0$ and $\vec{\omega}_0$ denote the HAT segment mass, inertia and angular velocity, respectively. All three parameters are expressed with respect to the inertial coordinate system. Normally, it is more convenient to describe the moment balance with respect to the local coordinate system of the HAT segment. The resulting equation is

$$\vec{R}_0^{iT}\vec{M}_{\rm hip} + \vec{R}_0^{iT}\vec{M}_{\rm sh} - (\vec{R}_0^{iT}\vec{F}_{\rm hip}) \times \vec{r}_{i,\rm hip} - (\vec{R}_0^{iT}\vec{F}_{\rm sh}) \times \vec{r}_{i,\rm sh} - (\vec{R}_0^{iT}\vec{F}_{\rm robo}) \times \vec{r}_{i,\rm hip} = \vec{I}_i\dot{\vec{\omega}}_i + \vec{\omega}_i \times (\vec{I}_i\vec{\omega}_i) \tag{3}$$

In (3), the inertial tensor $\vec{I}_{\rm i}$ and the vectors $\vec{r}_{i,\rm hip}, \vec{r}_{i,\rm sh}$ represent parameters expressed in the HAT coordinate system and are thus constant. The relation between the inertial and the local coordinate system is described by the homogenous rotational matrix $\vec{R}_0^i$.

According to the second Newton's law of motion, Eqs. (1)–(3) must be satisfied in each time instant. Formulating vector equations along horizontal and vertical directions, and expressing the components of the robot support, we get the algorithm for determining the desired robot supportive force. The supportive force can be expressed when all other variables and parameters in equations are known. Parameters of the body segments (masses, center-of-mass positions) can be estimated using anthropometric data [11], while the shoulder and hip forces and moments need to be assessed via the inverse dynamic approach utilizing the force reactions and kinematic measurements. Assessment of the foot and arm reactions requires utilization of multidimensional force sensors (robot force wrists, force plates or shoe insoles), while the motion kinematics can be assessed by an optical system or combination of simpler sensors. For example, lower extremity joint angles can be estimated from information about the robot end-point and foot positions, while HAT acceleration and angular velocity can be acquired using accelerometers and a gyroscope attached to the trunk.

3.1. Extended Kalman filter algorithm

For relating (1) and (3), an extended Kalman filter (EKF) algorithm was employed. Kalman filtering is a common approach in multisignal integration tasks relying on an approximate analytical model of the system [12]. In the EKF, the model is represented by a non-linear state space description incorporating state and measurement difference equations:

$$\vec{x}_{k+1} = \vec{f}(\vec{x}_k, \vec{u}_k, \vec{w}_k) \tag{4}$$

$$\vec{z}_k = \vec{h}(\vec{x}_k, \vec{v}_k) \tag{5}$$

In (4) the non-linear function $\vec{f}$ relates the state vector $\vec{x}$ and the input vector $\vec{u}$ at time step k to the state at step $k+1$. The measurement vector $\vec{h}$ in (5) relates the state to the measurements $\vec{z}_k$. Vectors $\vec{w}_k$ and $\vec{v}_k$ denote the superimposed process and measurement noise, respectively.

We defined the state vector as $\vec{x}_k = [\phi\,\dot{\phi}\,\ddot{\phi}\,A_y\,A_z\,f_{y,\rm robo}\,f_{z,\rm robo}]^{\rm T}$, where ϕ stands for the trunk inclination angle, A_y and A_z for the vertical and horizontal accelerations, and $f_{y,\rm robo}$ and $f_{z,\rm robo}$ for the trunk vertical and horizontal robot supportive force. Measurement vector $\vec{z}_k = [\dot{\phi}\,a_y\,a_z\,f_{y,\rm sh}\,f_{z,\rm sh}\,f_{y,\rm hip}\,f_{z,\rm hip}\,m_{x,\rm sh}\,m_{x,\rm hip}]^{\rm T}$ incorporates all the measurement values. Trunk inclination rate $\dot{\phi}$ and accelerations a_y, a_z are supposed to be measured by a gyroscope and accelerometers attached to the trunk. The shoulder and hip reactions $(f_{y,\rm sh}, f_{z,\rm sh}, f_{y,\rm hip}, f_{z,\rm hip}, m_{x,\rm sh}, m_{x,\rm hip})$ are assessable by an inverse dynamics calculation for the lower extremities. Motion kinematics and reaction forces need to be measured for this purpose. The particular functions of the state and measurement equation (4) and (5) are derived in Appendix A.

The discrete-time EKF algorithm is implemented as in [13]. The complete set of equations is shown below. The

EKF measurement update equations are

$$K_k = P_k^- H_k^T (H_k P_k^- H_k^T + R_k)^{-1} \tag{6}$$

$$\hat{\vec{x}}_k = \hat{\vec{x}}_k^- + K(\vec{z}_k - \vec{h}(\hat{\vec{x}}_k^-, 0)) \tag{7}$$

$$P_k = (I - K_k H_k) P_k^- \tag{8}$$

while the EKF time update equations are as follows:

$$P_{k+1}^- = A_k P_k A_k^T + Q_k \tag{9}$$

$$\hat{\vec{x}}_{k+1}^- = \vec{f}(\hat{\vec{x}}_k, \vec{u}_k, 0) \tag{10}$$

The EKF propagates the state and error covariance estimates (10) and (9) by computing the filter gain matrix (6), and by updating the state and covariance estimates based on the measurement residual (7) and (8). Matrices A_k and H_k are computed by linearizing (15) and (16) around $\hat{\vec{x}}_k^-$ prediction at each time step. Matrices A and H are the Jacobian matrices of partial derivatives of $\vec{f}()$ and $\vec{h}()$ with respect to vector $\vec{x}$:

$$A_k = \frac{\partial f_i}{\partial x_j}(\vec{x}_k, \vec{u}_k, 0), \qquad H_k = \frac{\partial h_i}{\partial x_j}(\vec{x}_k, 0) \tag{11}$$

The filter is initialized with a state estimate corresponding to the true state and a large covariance matrix.

4. Evaluation of the proposed PDRAMA control approach

The PDRAMA control approach proposal was evaluated by a simulation study. For this purpose, the standing-up manoeuvre of a paraplegic subject was modelled in a simulation environment. In the simulation model, the models of voluntary activity, robot support and dynamics of human body motion were incorporated. The simulation model was built on the basis of measurement data acquired in the actual standing-up trials of a paraplegic subject.

4.1. Measurement of actual standing-up trials of a paraplegic subject

In order to acquire measurement data of the standing-up of an disabled individual, several experimental standing-up trials were accomplished. In the experiments, a person with paraplegia was involved (subject MT, female, 30 years, 171 cm, 75 kg, injury level T 4-5).

In Fig. 3, the experimental set-up is shown incorporating the robot-assistive device and the arm supportive frame. The forces on the arm support were measured by a six-axis JR3 robot wrist sensor, while the foot reactions were assessed by the AMTI force plate. Motion of body segments was measured with an Optotrak-Northern Digital optical system, which measures the three-dimensional positions of active markers (infrared LEDs).

Prior to the measurements, three unsupported standing-up trials had been performed to relieve spasticity in the paralyzed extremities and familiarize the subject with the measuring equipment. In the following unsupported trial, the hip joint trajectory was recorded for the purpose of usage in the later robot-assisted standing-up as a desired seat trajectory. The trunk position and orientation were also recorded to be used as a reference in the simulated standing-up.

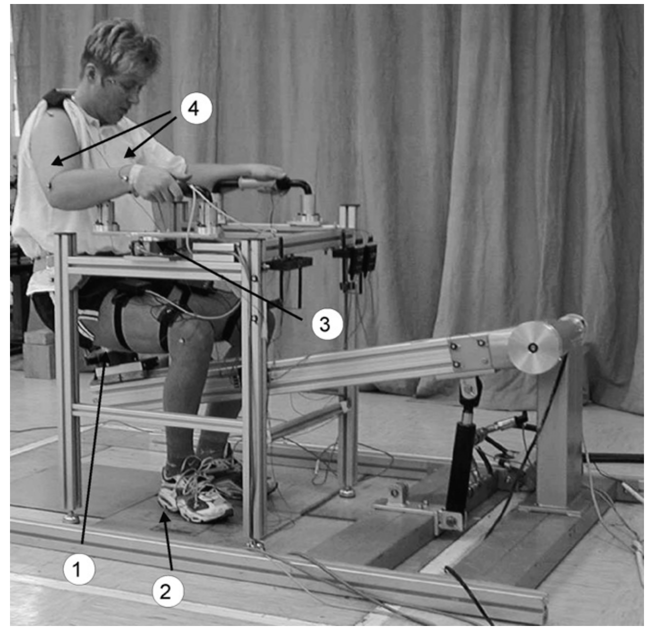

Fig. 3. Paraplegic subject in the standing-up measurement set-up: (1) seat reaction force sensor; (2) feet reaction force plates; (3) arm reaction force sensor; (4) infrared markers.

In the robot-supported trials of standing-up, the robot device was operating in the position control mode. No interaction control was involved in this regime. Motion was initiated by the patient via a push button mounted on the walker handle. After triggering, the robot accomplished motion along the desired seat trajectory, while the subject was trying to adapt to the imposed hip position. The body motion kinematics and interaction forces were acquired in each standing-up trial. The hip and shoulder forces were determined off-line via the inverse dynamics calculation.

4.2. Simulation environment

In the simulation study, the motion of the human body in the standing-up process was simulated in the Matlab–Simulink software environment (see Fig. 4). A dynamic model of the human body was integrated into the Simulink via an S-function interface. The dynamic model was developed by the use of the SD-FAST software package (Symbolic Dynamics Inc.) and included three rigid body segments – shanks, thighs and HAT – constrained to sagittal plane motion. In the model the human body anthropometric parameters [11], the visco-elastic properties of the joints [14] and the human voluntary control were incorporated. As with para-

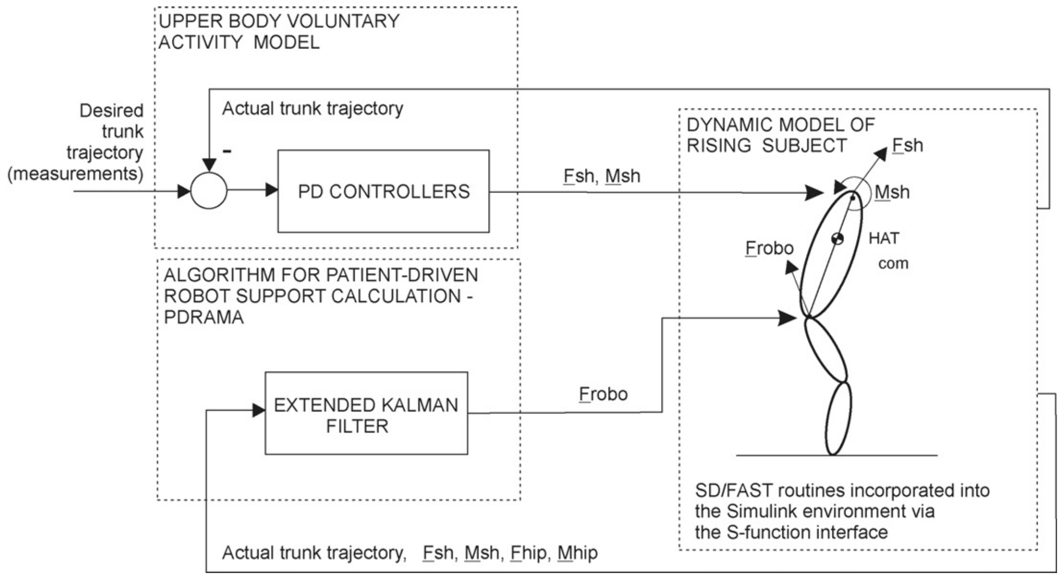

Fig. 4. Block scheme of simulation concept.

plegic subjects, no active moments were applied in the lower extremities.

Human volition was modelled with the assumption that during standing-up movements subjects try to follow a trajectory they learned from past movements. Paraplegic patients due to limited leg joint moments are able to utilize only arm support for maintaining balance and sustaining the desired movement. Assuming this behavior we developed a simple tracking controller to model the patient's voluntary upper body effort. The controller generates the shoulder forces and moment with objective to minimize the deviations from the desired trunk motion trajectory that had been obtained from an experiment of the actual unsupported standing-up as explained in Section 4.1. A similar approach for modelling the voluntary activity in standing-up in paraplegia was taken in [8] and [15]. The trajectory-tracking controller was realized as three DOF decentralized proportional-derivative (PD) tracking controller for controlling the vertical and horizontal shoulder forces, and shoulder moment. The controller configuration was chosen with regards to the examples from robot control. The approach is known as global asymptotically stable in trajectory tracking [16]. The controller gain values were tuned by the help of Simulink response optimization toolbox, which attempts to satisfy the constraints on the response signals within Simulink models by adjusting the tuned parameters. In our case, the motion response was constrained to track and closely match the reference trunk motion trajectory while the profile of shoulder forces was simultaneously constrained within a time-domain window. Two different optimization approaches were implemented. First, the pattern search method was applied for finding the approximate values, and the gradient descent method was used for fine tuning, afterwards.

In simulation, the unsupported standing-up was facilitated by arm support only, while in supported standing-up, in each integration step, the supportive force was determined by the Kalman filter algorithm and applied as an external force vector at the hip joint mimicking the robot support.

4.3. Evaluation of simulation model

The simulation model of the standing-up manoeuvre was evaluated by comparison with the measurement data. The unsupported standing-up trial was chosen for comparison. For the simulation model, the human body parameters (mass, inertia, segment length) were determined according to the anthropometry of the participating subject. The desired trunk trajectory fed to the input of the voluntary activity controller was acquired from the measurement data. In Fig. 5, voluntary activity and body position at particular time instants are compared in simulated and actual standing-up. Upper body voluntary activity is represented by three graphs showing shoulder moment in the sagittal plane, shoulder horizontal force and shoulder vertical force. The position of the body is illustrated by the dark and white stick figures representing the position at particular time instants in simulated and actual standing-up, respectively.

From Fig. 5, it is evident that good agreement between simulated and actual standing-up manoeuvres is achieved. The model rises from sitting to standing position in the same time sequence using almost identical vertical supportive force pattern. Small difference is evident in trunk orientation, however the balancing horizontal shoulder force and sagittal moment stays in the same range as in actual standing-up. This proves that the simplified dynamic model of the human body and the model of voluntary activity approximate appropriately the behavior of the human body in rising.

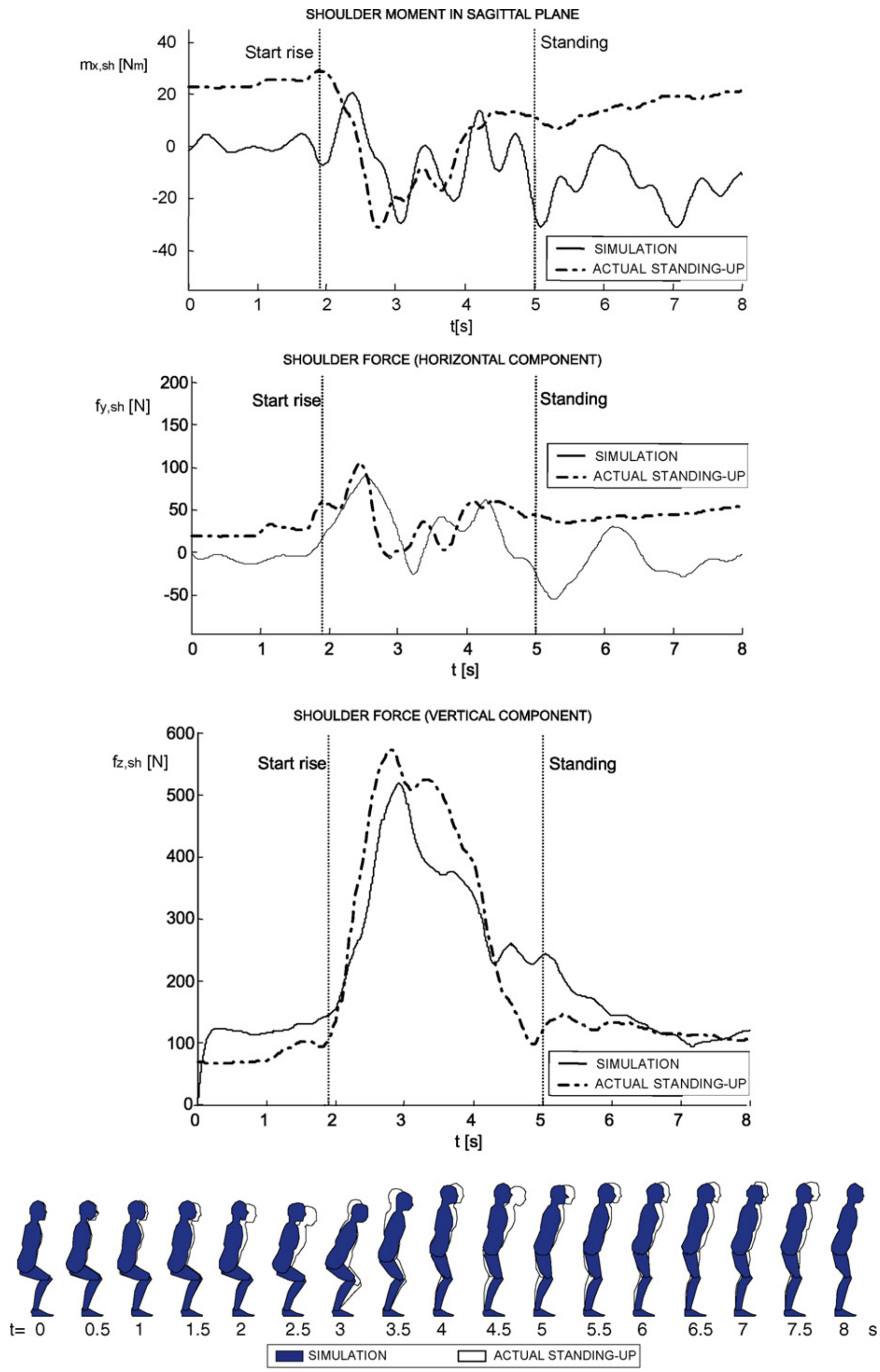

Fig. 5. Comparison of voluntary activity and body positions in simulated and actual standing-up of paraplegic subject.

5. Results

In the results, the robot-assisted standing-up of a paraplegic subject is analyzed. Two approaches to the robot control are compared. The actual standing-up facilitated by the position controlled robot device is compared to the simulated standing-up. In simulated standing-up, the model of the subject is supported by the force determined by the PDRAMA algorithm.

In Fig. 6, the upper body contributions to body weight support are shown for two examples of the robot-assisted standing-up. The graph presents the vertical component of the shoulder joint force. Below the graph, the body motion kinematics is presented by dark and white stick figures illustrating the simulated and actual standing-up examples. The arrows describe the amplitude and direction of the force acting in the shoulder joint. The line style of the arrows corresponds to the line style in the graph. In this way, Fig. 6 represents the

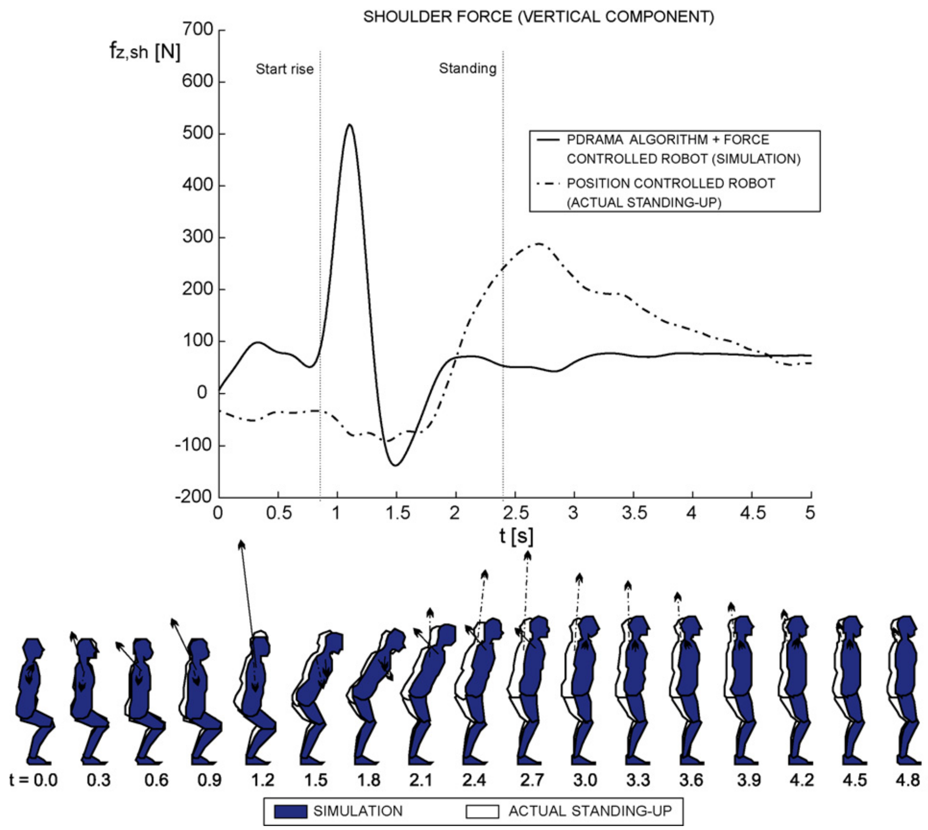

Fig. 6. Voluntary activity in robot-assisted standing-up: measured results (robot in position control mode) and simulation results (robot in force control mode, supportive force determined by the PDRAMA algorithm).

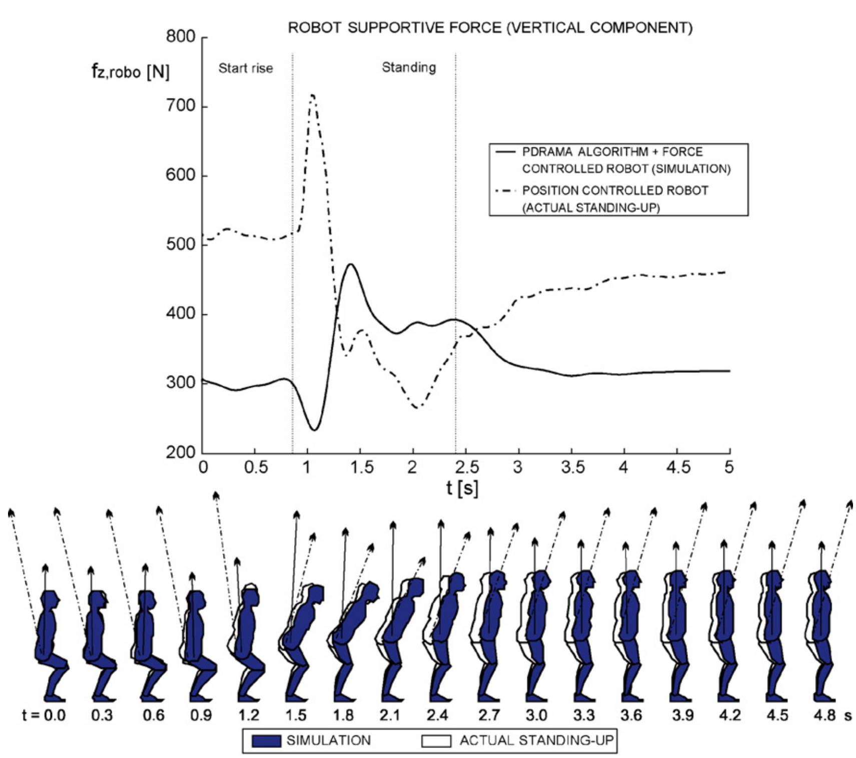

Fig. 7. Robot support in robot-assisted standing-up: measured results (robot in position control mode) and simulation results (robot in force control mode, supportive force determined by the PDRAMA algorithm).

voluntary activity of the subject during rising. Higher subject's activity in initiating the manoeuvre can be noticed in PDRAMA example. This implies to the patient-driven nature of standing-up.

Fig. 7 uses the same notation as the figure above and shows the robot interaction force in the same standing-up examples. The figure represents the robot assistance to the subject in the standing-up manoeuvre. It can be seen that high interaction between the subject and the robot at the beginning of standing-up is diminished in PDRAMA example. Moreover, stick figures show that robot supported the subject primarily in vertical direction. The observations prove the subject-following robot mode of operation provided by the PDRAMA control approach.

In the PDRAMA control approach, the robot supportive force is determined on the basis of foot and arm reaction forces. Scaling these forces before being fed to the controller varies the amount of the body weight support between the voluntary and the robot contributions. This effect opens the possibility for altering the training conditions in robot-assisted standing-up. In Fig. 8, three simulation examples of PDRAMA-driven standing-up with different feedback sensitivity settings for arm supportive force are presented. The upper graph shows the vertical shoulder force illustrating voluntary activity. The lower graph shows the vertical robot support. The scaling factor of the arm reaction force is denoted in the legend.

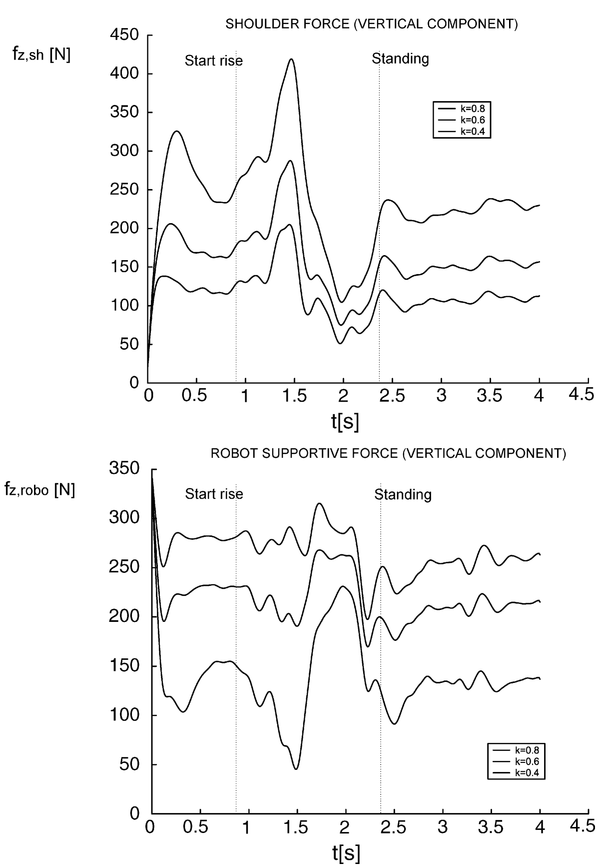

Fig. 8. Variation of training conditions achieved by different feedback sensitivity setting of arm reaction force in PDRAMA approach.

6. Discussion

The results demonstrate that both control approaches examined in the study are capable of assuring proper support to the subject to accomplish the rising manoeuvre. A similar standing-up motion pattern is demonstrated in both examples. However, from Figs. 6 and 7 a fundamental difference between the control approaches can be observed. In standing-up facilitated by the position-controlled robot device, a high peak in the subject–robot interaction force is noticed at the beginning of rising. The high interaction implies that the robot device acts as a master device, which imposes the motion to the subject. As a consequence, the low voluntary arm activity of the subject is present in body weight lifting. On the other side, in the PDRAMA simulation example, it is evident that the subject initiated and guided the motion by the upper body activity. The robot provided the needed support only. In this way, voluntary control over the motion manoeuvre is assured to the subject.

An improvement of the PDRAMA approach over the CHRELMS and PDMR is that the implementation of the algorithm does not require direct measurement of human motion kinematics. Measuring of human motion normally requires a sophisticated optical system and a complex measuring procedure preferably utilized in a laboratory environment. Instead, only the trunk inclination rate and translational accelerations need to be explicitly measured using a multidimensional sensor attached to the trunk. Assessment is additionally simplified since information about the robot end-effector position and information about the foot reaction force application point can be used to assess the motion of the lower extremity.

7. Conclusion

This paper presents a rehabilitation robot device intended for augmenting the human capabilities in the standing-up manoeuvre. For control, a novel algorithm is presented which incorporates human voluntary activity into the robot control scheme. The PDRAMA algorithm is designed to determine the interaction force between the subject and the robot, thus generating the reference to the robot explicit force controller. The paper presents the results of experimental and simulation testing in the robot-assisted standing-up of a paraplegic subject. The proposed PDRAMA control approach is compared to conventional position control. The results demonstrate the superior performance of the PDRAMA algorithm. The algorithm controls the robot motion without the need for specific reference defined. It accounts for the contributions from trunk inertia in dynamic motion and the contributions from the lower and upper extremities to body weight lifting forces.

In this way, a unique approach in rehabilitation robotics has been developed: a "patient-driven" control of robot-assisted training. Moreover, the PDRAMA control algorithm enables the alteration of body weight bearing portions between the robot and the subject. Thus, the standing-up training regime can be varied, depending on the subject's etiology, from more "robot-driven" at the beginning of rehabilitation, to more and more "patient-driven" in accordance with the patients's progress. The sensory system needed for the PDRAMA operation is practical for implementation. Providing measuring data, the robot device is applicable in the function of an assistive device as well as an assessment tool. This opens a range of possible applications of the PDRAMA-driven robot device in clinical praxis.

Acknowledgement

The authors acknowledge the Republic of Slovenia Ministry of Education, Science and Sport grant *Motion Analysis and Synthesis in Human and Machine* (P2-0228 C).

Appendix A

The appendix derives the vector HAT balance equations (1) and (3) along horizontal and vertical direction. From obtained result, the components of the EKF state and measurement vectors are expressed and written in vector form.

The derivations of HAT force balance equation (1) along horizontal and vertical direction are

$$f_{y,\mathrm{hip}} + f_{y,\mathrm{sh}} + f_{y,\mathrm{robo}} = A_y m_{\mathrm{hat}} \tag{12}$$

$$f_{z,\mathrm{hip}} + f_{z,\mathrm{sh}} - m_{\mathrm{hat}} g + f_{z,\mathrm{robo}} = A_z m_{\mathrm{hat}} \tag{13}$$

while the HAT moment balance equation (3) describing only the balance in sagittal plane is

$$\begin{aligned} &m_{x,\mathrm{hip}} + m_{x,\mathrm{sh}} - r_{z,\mathrm{hip}} \cos\phi f_{y,\mathrm{hip}} + r_{y,\mathrm{hip}} \cos\phi f_{z,\mathrm{hip}} \\ &\quad - r_{y,\mathrm{hip}} f_{y,\mathrm{hip}} \sin\phi - r_{z,\mathrm{hip}} f_{z,\mathrm{hip}} \sin\phi + \cos\phi f_{z,\mathrm{sh}} r_{y,\mathrm{sh}} \\ &\quad - \cos\phi f_{y,\mathrm{sh}} r_{z,\mathrm{sh}} - f_{y,\mathrm{sh}} r_{y,\mathrm{sh}} \sin\phi - f_{z,\mathrm{sh}} r_{z,\mathrm{sh}} \sin\phi \\ &\quad - r_{z,\mathrm{robo}} \cos\phi f_{y,\mathrm{robo}} + r_{y,\mathrm{robo}} \cos\phi f_{z,\mathrm{robo}} \\ &\quad - r_{y,\mathrm{robo}} f_{y,\mathrm{robo}} \sin\phi - r_{z,\mathrm{robo}} f_{z,\mathrm{robo}} \sin\phi = i_x \ddot{\phi} \end{aligned} \tag{14}$$

The particular functions of the state equation (4) derived from (12), (13) and (14) are then given as

$$\begin{bmatrix} f_1 \\ f_2 \\ f_3 \\ f_4 \\ f_5 \\ f_6 \\ f_7 \end{bmatrix} = \begin{bmatrix} \phi \\ \dot{\phi} \\ \ddot{\phi} \\ A_y \\ A_z \\ f_{y,\mathrm{robo}} \\ f_{z,\mathrm{robo}} \end{bmatrix} = \begin{bmatrix} \phi + \dot{\phi}\,\mathrm{d}t \\ \dot{\phi} + \ddot{\phi}\,\mathrm{d}t \\ (-r_{z,\mathrm{hip}} \cos\phi f_{y,\mathrm{hip}} + r_{y,\mathrm{hip}} \cos\phi f_{z,\mathrm{hip}} - r_{z,\mathrm{robo}} \cos\phi f_{y,\mathrm{robo}} + r_{y,\mathrm{robo}} \cos\phi f_{z,\mathrm{robo}} + m_{x,\mathrm{hip}} \\ + m_{x,\mathrm{sh}} + \cos\phi f_{z,\mathrm{sh}} r_{y,\mathrm{sh}} - \cos\phi f_{y,\mathrm{sh}} r_{z,\mathrm{sh}} - r_{y,\mathrm{hip}} f_{y,\mathrm{hip}} \sin\phi - r_{z,\mathrm{hip}} f_{z,\mathrm{hip}} \sin\phi \\ - r_{y,\mathrm{robo}} f_{y,\mathrm{robo}} \sin\phi - r_{z,\mathrm{robo}} f_{z,\mathrm{robo}} \sin\phi - f_{y,\mathrm{sh}} r_{y,\mathrm{sh}} \sin\phi - f_{z,\mathrm{sh}} r_{z,\mathrm{sh}} \sin\phi)/i_{x,\mathrm{hat}} \\ (f_{y,\mathrm{hip}} + f_{y,\mathrm{robo}} + f_{y,\mathrm{sh}})/m_{\mathrm{hat}} \\ (f_{z,\mathrm{hip}} + f_{z,\mathrm{robo}} + f_{z,\mathrm{sh}} - g m_{\mathrm{hat}})/m_{\mathrm{hat}} \\ A_y m_{\mathrm{hat}} - f_{y,\mathrm{hip}} - f_{y,\mathrm{sh}} \\ m_{\mathrm{hat}} g + A_z m_{\mathrm{hat}} - f_{z,\mathrm{hip}} - f_{z,\mathrm{sh}} \end{bmatrix} \tag{15}$$

and the non-linear measurement equation (5) takes the form:

$$\begin{bmatrix} h_1 \\ h_2 \\ h_3 \\ h_4 \\ h_5 \\ h_6 \\ h_7 \\ h_8 \\ h_9 \end{bmatrix} = \begin{bmatrix} \dot{\phi} \\ a_y \\ a_z \\ f_{y,\mathrm{sh}} \\ f_{z,\mathrm{sh}} \\ f_{y,\mathrm{hip}} \\ f_{z,\mathrm{hip}} \\ m_{x,\mathrm{sh}} \\ m_{x,\mathrm{hip}} \end{bmatrix} = \begin{bmatrix} \dot{\phi} \\ A_y \cos\phi + A_z \sin\phi \\ -A_y \sin\phi + A_z \cos\phi \\ A_y m_{\mathrm{hat}} - f_{y,\mathrm{robo}} - f_{y,\mathrm{hip}} \\ m_{\mathrm{hat}} g + A_z m_{\mathrm{hat}} - f_{z,\mathrm{robo}} - f_{z,\mathrm{hip}} \\ A_y m_{\mathrm{hat}} - f_{y,\mathrm{sh}} - f_{y,\mathrm{robo}} \\ m_{\mathrm{hat}} g + A_z m_{\mathrm{hat}} - f_{z,\mathrm{sh}} - f_{z,\mathrm{robo}} \\ i_x \ddot{\phi} + r_{z,\mathrm{hip}} \cos\phi f_{y,\mathrm{hip}} - r_{y,\mathrm{hip}} \cos\phi f_{z,\mathrm{hip}} + r_{z,\mathrm{robo}} \cos\phi f_{y,\mathrm{robo}} - r_{y,\mathrm{robo}} \cos\phi f_{z,\mathrm{robo}} \\ - m_{x,\mathrm{hip}} - \cos\phi f_{z,\mathrm{sh}} r_{y,\mathrm{sh}} + \cos\phi f_{y,\mathrm{sh}} r_{z,\mathrm{sh}} + r_{y,\mathrm{hip}} f_{y,\mathrm{hip}} \sin\phi + r_{z,\mathrm{hip}} f_{z,\mathrm{hip}} \sin\phi \\ + r_{y,\mathrm{robo}} f_{y,\mathrm{robo}} \sin\phi + r_{z,\mathrm{robo}} f_{z,\mathrm{robo}} \sin\phi + f_{y,\mathrm{sh}} r_{y,\mathrm{sh}} \sin\phi + f_{z,\mathrm{sh}} r_{z,\mathrm{sh}} \sin\phi \\ i_x \ddot{\phi} + r_{z,\mathrm{hip}} \cos\phi f_{y,\mathrm{hip}} - r_{y,\mathrm{hip}} \cos\phi f_{z,\mathrm{hip}} + r_{z,\mathrm{robo}} \cos\phi f_{y,\mathrm{robo}} - r_{y,\mathrm{robo}} \cos\phi f_{z,\mathrm{robo}} \\ - m_{x,\mathrm{sh}} - \cos\phi f_{z,\mathrm{sh}} r_{y,\mathrm{sh}} + \cos\phi f_{y,\mathrm{sh}} r_{z,\mathrm{sh}} + r_{y,\mathrm{hip}} f_{y,\mathrm{hip}} \sin\phi + r_{z,\mathrm{hip}} f_{z,\mathrm{hip}} \sin\phi \\ + r_{y,\mathrm{robo}} f_{y,\mathrm{robo}} \sin\phi + r_{z,\mathrm{robo}} f_{z,\mathrm{robo}} \sin\phi + f_{y,\mathrm{sh}} r_{y,\mathrm{sh}} \sin\phi + f_{z,\mathrm{sh}} r_{z,\mathrm{sh}} \sin\phi \end{bmatrix} \tag{16}$$

References

[1] Kralj A, Bajd T. Functional electrical stimulation: standing and walking after spinal cord injury. Boca Raton, Florida: CRC Press; 1989.
[2] Bajd T, Kralj A, Turk R. Standing-up of a healthy subject and a paraplegic patient. J Biomech 1982;15(1):1–10.
[3] Schüldt K, Ekholm J, Németh G, Arborelius U, Harms-Ringdahl K. Knee load and muscle activity during exercises in rising. Scand J Rehabil Med 1983;15(Suppl 9):174–99.
[4] Riener R, Ferrarin M, Pavan E, Frigo C. Patient-driven control of FES-supported standing up and sitting down: experimental results. IEEE Trans Rehabil Eng 2000;8(4):523–9.
[5] Kamnik R, Bajd T. Standing-up robot: an assistive rehabilitative device for training and assessment. J Med Eng Technol 2004;28(2):74–80.
[6] Hogan N. Impedance control: an approach to manipulation: parts I, II, III. J Dyn Syst Meas Contr 1985;107(1):1–24.
[7] Kamnik R, Matko D, Bajd T. Application of model reference adaptive control to industrial robot impedance control. J Intell Robot Syst 1998;22(2):153–63.
[8] Riener R, Fuhr T. Patient-driven control of FES-supported standing up: a simulation study. IEEE Trans Rehabil Eng 1998;6(2):113–24.
[9] Donaldson NdeN, Yu C-H. Experiments with CHRELMS patient-driven stimulator controllers for the restoration of function to paralysed legs. Proc Inst Mech Eng, H J Eng Med 2000;214(1):1–20.
[10] Mattila J, Virvalo T. Energy-efficient motion control of a hydraulic manipulator. In: Proceedings of the 2000 IEEE international conference on robotics and automation (ICRA'2000); 2000, p. 3000–6.
[11] Leva PD. Adjustments to Zatsiorksy-Seluyanov's segment inertia parameters. J Biomech 1996;29(9):1223–30.
[12] Brown R, Hwang P. Introduction to random signals and applied Kalman filtering. New York, USA: John Wiley & Sons; 1997.
[13] Julier S, Uhlman J, Durrant-Whyte H. A new approach for filtering nonlinear systems. In: Proceedings of the 1995 American control conference; 1995, p. 1628–32.
[14] Riener R, Edrich T. Identification of passive elastic joint moments in the lower extremities. J Biomech 1999;32(5):539–44.
[15] Davoodi R, Kamnik R, Andrews B, Bajd T. Predicting the voluntary arm forces in FES-assisted standing up using neural networks. Biol Cybern 2001;85(2):133–43.
[16] Sciavicco L, Siciliano B. Modelling and control of robot manipulators. London, GB: Springer; 2000.